

# Lawrence Berkeley National Laboratory

## Recent Work

### Title

GERMANIUM PET u A NOVEL LOW-NOISE ACTIVE DEVICE

### Permalink

<https://escholarship.org/uc/item/50n8k88f>

### Authors

Elad, Emanuel  
Nakamura, Michiyuki.

### Publication Date

1967-09-01

C.?

# University of California Ernest O. Lawrence Radiation Laboratory

GERMANIUM FET--A NOVEL LOW-NOISE ACTIVE DEVICE

Emanuel Elad and Michiyuki Nakamura

September 1967

RECEIVED  
LAWRENCE  
RADIATION LABORATORY

SEP 20 1967  
LIBRARY AND  
DOCUMENTS

TWO-WEEK LOAN COPY

This is a Library Circulating Copy  
which may be borrowed for two weeks.  
For a personal retention copy, call  
Tech. Info. Division, Ext. 5545

UCRL-17818  
eg. 2

## **DISCLAIMER**

This document was prepared as an account of work sponsored by the United States Government. While this document is believed to contain correct information, neither the United States Government nor any agency thereof, nor the Regents of the University of California, nor any of their employees, makes any warranty, express or implied, or assumes any legal responsibility for the accuracy, completeness, or usefulness of any information, apparatus, product, or process disclosed, or represents that its use would not infringe privately owned rights. Reference herein to any specific commercial product, process, or service by its trade name, trademark, manufacturer, or otherwise, does not necessarily constitute or imply its endorsement, recommendation, or favoring by the United States Government or any agency thereof, or the Regents of the University of California. The views and opinions of authors expressed herein do not necessarily state or reflect those of the United States Government or any agency thereof or the Regents of the University of California.

Presented at the 14th Nuclear Science Symposium  
of the IEEE, Los Angeles, California  
October 31-November 2, 1967

UCRL-17818  
Preprint

UNIVERSITY OF CALIFORNIA

Lawrence Radiation Laboratory  
Berkeley, California

AEC Contract No. W-7405-eng-48

GERMANIUM FET--A NOVEL LOW-NOISE ACTIVE DEVICE

Emanuel Elad and Michiyuki Nakamura

September 1967

GERMANIUM FET--A NOVEL LOW-NOISE ACTIVE DEVICE

Emanuel Elad and Michiyuki Nakamura

Lawrence Radiation Laboratory  
University of California  
Berkeley, California

Abstract

A novel device for low-noise amplification--the germanium junction field-effect transistor (JFET)--is introduced. The properties of germanium and silicon at cryogenic temperatures are summarized. Based on the conclusions of this summary, a theoretical comparison between germanium and silicon JFET's is made, followed by a comparison of commercially available JFET's from both materials.

A low-noise preamplifier featuring liquid-helium-cooled germanium JFET's was built and operated with semiconductor radiation detectors. Pulse generator resolution of the preamplifier for zero external capacitance is 0.28 keV FWHM (Ge) with a slope of 0.018 keV/pF. Actual resolution obtained with the silicon detector for low-energy x rays is 0.37 keV.

I. Introduction

The development of semiconductor radiation detectors triggered a continuous search for lower-and-lower noise preamplifiers, to take full advantage of the excellent resolution of these detectors. During the last few years, the main effort was concentrated on the input stage, which apart from the detector itself, is the most important factor in determining the resolution of the spectrometer. In the input stage, various active elements and different configurations were investigated. Following the technological progress came the use of vacuum tubes,<sup>1,2</sup> bipolar transistors,<sup>3,4</sup> tunnel diodes,<sup>5</sup> and silicon junction field-effect transistors.<sup>6</sup> However, only special low-noise vacuum tubes and field-effect transistors (FET) got beyond the experimental stage.

The vacuum tube and the early noncooled FET preamplifiers had equivalent noise charge (ENC) between 250 and 500 electrons rms. The inherent temperature dependence of semiconductors stimulated the search for a temperature at which FET's exhibit their optimum signal-to-noise ratio. This optimum temperature, which nearly coincides with the temperature required to obtain maximum transconductance ( $g_m$ ), depends on the impurity concentration and is reported to be in the range of 100 to 140°K for silicon n-channel FET's. Several preamplifiers, based on cooled FET's were built, the most recent ones utilizing well-optimized n-channel silicon devices having high values of  $g_m/C_g$ .<sup>7-9</sup> These preamplifiers had ENC's between 50 and 60 electrons rms with a slope of 4 to 5 electrons/pF.

This paper introduces the germanium junction FET (JFET) as the active element of a low-noise input stage. This device provides high gain coupled with very low noise when operated at 4.2°K. Using the only commercially available germanium FET type TIX301 (or TIXM12--a plastic-encapsulated version of TIX301), we obtained an ENC of 40 electrons rms [0.28 keV FWHM (Ge)] with a slope of 2.5 electrons/pF (0.018 keV/pF). Besides the high resolution coupled with low sensitivity to capacitance, the germanium JFET offers two more advantages over its silicon counterpart. One is simple selection of low-noise units performed at room temperature, and the other, no requirement for special temperature adjustment, as the optimum temperature of the germanium JFET's is in vicinity of the boiling point of liquid helium.

The described preamplifier was tested with a low-capacitance silicon detector, and low-energy x rays were measured with 0.37-keV resolution. Further improvements of resolution are expected with the technological progress in fabrication of germanium FET's.

II. Germanium Versus Silicon at Cryogenic Temperatures

The elemental semiconductors, germanium and silicon, are the basic materials of modern electronic devices. The properties of these materials were carefully studied and tabulated. Some of the relevant parameters of germanium and silicon are given in Table I.<sup>10</sup>

Table I. Parameters of germanium and silicon.<sup>10</sup>

	Energy gap (eV)		Ionization energy of impurities (eV)		Relative dielectric constant $\epsilon/\epsilon_0$	Effective mass ratio $m^*/m_0$	
	(0°K)	(300°K)	P	B		holes	electrons
Ge	0.744	0.67	0.012	0.0104	16	0.37	0.55
Si	1.153	1.107	0.044	0.046	12	0.59	1.1

In this article we will be concerned with the temperature behavior of JFET's and its dependence on the electrical conductivity of the channel (see Section III). The electrical conductivity  $\sigma$  of an extrinsic semiconductor depends on the mobility and density of free carriers as expressed by the formula (for the n type)

$$\sigma = q\mu_e n, \quad (1)$$

where  $n$  is the density of free electrons,  $\mu_e$  is the electron mobility, and  $q$  is the charge of an electron.

Let us review now the temperature dependence of these two parameters. For elemental semiconductors, scattering by acoustic phonons and ionized impurities limits the mobilities of the free carriers. The mobility limited by the acoustic modes of lattice vibration ( $\mu_\ell$ ) has the temperature dependence.

$$\mu_\ell = Am^{*-5/2} T^{-3/2}, \quad (2)$$

where  $A$  is a numerical constant,  $m^*$  is the effective mass, and  $T$  is the absolute temperature.

The mobility limited by the scattering action of ionized impurities is

$$\mu_i = Bm^{*-1/2} N^{-1} T^{3/2}, \quad (3)$$

where  $B$  is a proportionality constant that varies very slowly with temperature as  $\log(T/T_0)$ , and  $N$  is the impurity concentration. The total mobility  $\mu$  is given by

$$\frac{1}{\mu} = \frac{1}{\mu_\ell} + \frac{1}{\mu_i}, \quad (4)$$

with the assumption that the relaxation times resulting from the two scattering mechanisms have the same energy dependence. From Eq. (4) we see that the mobility will be determined by the smaller of its two components. The opposite temperature dependence of the two scattering mechanisms as expressed in Eq. (2) and (3) points to the existence of a maximum in the mobility-temperature curve. The maximum point ( $T_m$ ) depends on impurity concentration, effective mass, and the coefficients  $A$  and  $B$ . Above the temperature  $T_m$  (room temperature included), the mobility is determined by lattice scatterings, and below  $T_m$ , by impurity scattering. Room temperature mobilities in germanium are higher than those in silicon, because of the lower effective mass of the carriers in germanium (see Table I). The lower effective mass and the relative values of the constants  $A$  and  $B$  in germanium<sup>11</sup> make lattice scattering dominant down to very low temperatures. Therefore we conclude that maximum mobility in germanium is attained at lower temperatures than in silicon, and its value is higher than that of silicon. These conclusions are in good agreement with the experimental data (Fig. 1) gathered by several researchers.

The density of free electrons in a n-type uncompensated semiconductor is

$$n = \left(\frac{N_c N}{2}\right)^{1/2} \exp\left(-\frac{E_d}{2kT}\right), \quad (5)$$

where

$$N_c = 2 \left(\frac{2\pi m_e^* kT}{h^2}\right)^{3/2}. \quad (6)$$

Here  $N$  is the impurity concentration,  $E_d$  is the ionization energy of the impurities,  $k$  is Boltzman's constant, and  $h$  is Planck's constant.

The main temperature dependence of  $n$  is through  $\exp(-E_d/2kT)$ . The importance of the ratio, (ionization energy)/(thermal energy), is clearly manifested. The ionization energies of the common impurities in germanium are about one-fourth of their corresponding values in silicon (see Table I). Thus the density of free carriers in germanium at cryogenic temperatures is higher than that in silicon.

From the temperature dependence of the mobility and the density of free carriers in germanium and silicon we can conclude that for equal impurity concentrations the maximum conductivity of germanium will be higher and will be attained at lower temperature. The reported experimental data, summarized in Fig. 2, confirm this conclusion (no data was found on p-type germanium in the discussed temperature region).

### III. Germanium and Silicon JFET's at Cryogenic Temperatures

Junction field-effect transistors operate through modulation of a current path by a depletion region of a reverse-biased p-n junction. Their principles of operation and characteristics are described in most books on semiconductor devices. For an abrupt-gate junction device, the saturation current is given by

$$I_{sat} = \frac{g_0 V_p}{3} \left[ 1 - 3\frac{V_g}{V_p} + 2\left(\frac{V_g}{V_p}\right)^{3/2} \right], \quad (7)$$

where  $g_0$  is the conductance of the metallurgical channel,  $V_p$  is the pinch-off voltage, and  $V_g$  is the gate voltage. An important parameter of a JFET is its transconductance,

$$g_m = \left| \frac{\partial I_{sat}}{\partial V_g} \right| = g_0 \left[ 1 - \left(\frac{V_g}{V_p}\right)^{1/2} \right]. \quad (8)$$

Maximum transconductance occurs at  $V_g = 0$ , i.e.,

$$g_m(\max) = g_0. \quad (9)$$

Thus it is clear that the temperature behavior of  $g_m$  will follow that of the conductance of the channel. Based on the conclusions of the previous section, we see that germanium JFET's should exhibit higher  $g_m$ 's at cryogenic temperatures.

The main noise source of JFET's is the thermal noise of the conducting channel.<sup>12</sup> This source can be represented by the following voltage generator at the input

$$\left(\frac{2}{e g}\right)^{1/2} = \left(\frac{8kT\Delta f}{3g_m}\right)^{1/2} \quad (10)$$

where  $\Delta f$  is a small frequency interval. From Eq. (10) we see that the noise of a JFET can be reduced by lowering the temperature or increasing the  $g_m$ . Therefore, we can conclude that the minimal thermal noise of germanium JFET's will be significantly smaller than that of their silicon counterparts, because of their higher  $g_m$  which is attained at lower temperatures.

The thermal noise of the channel is singled out neglecting, among others, the shot noise generated in the gate junction. The assumption is certainly in error for germanium JFET's operating at 300°K, but is close to reality for their operation at 4.2°K.

It is well known that the ohmic source resistance reduces the effective  $g_m$  of an FET and constitutes a source of thermal noise. Both parasitic effects are small in germanium FET's operating at 4.2°K.

The signal-to-noise ratio of an FET stage when used in conjunction with a p-i-n radiation detector, depends on the input capacitance of the FET. This in turn is the capacitance of the reverse-biased gate junction given by

$$C = A \left[ \frac{q\epsilon\epsilon_0 N}{2(\psi_0 - V)} \right]^{1/2} \quad (11)$$

where  $A$  is the area of the junction,  $\epsilon\epsilon_0$  is the dielectric constant,  $\psi_0$  is the built-in voltage, and  $V$  is the external bias. The capacitance is weakly temperature-dependent through  $\psi_0$  and the ionized impurity concentration  $N$ . The latter decrease mainly at the very low temperatures; overall the capacitance decreases with temperature. For the FET stage it means further improvement of its signal-to-noise ratio. Germanium junctions will have slightly higher capacitance per unit area due to the higher dielectric constant of germanium over silicon (Table I).

#### IV. Commercial Germanium Versus Silicon JFET's

During the last three years the commercial silicon JFET line expanded rapidly, offering a large variety of devices with high  $g_m/C_g$  ratios. The emphasis has been placed on n-channel units having the inherent advantage of higher electron mobility. Some of the more popular types used in low-noise amplifiers include 2N3823 (Texas Instruments), 2N4416 (Union Carbide), and recently 2N5105 (Amperex). The transconductance of these devices at room temperature is between

3.5 and 5 mA/V increasing to 7 to 9 mA/V at the optimum temperature which ranges from 100 to 140°K. The transconductance versus temperature curve (2N3823) shown in Fig. 3, represents the typical variation of  $g_m$  for silicon JFET's. Notice the strong decrease of  $g_m$  below the optimum temperature, reaching zero at 50°K. This is in good agreement with the variation of conductivity of the metallurgical channel [see Fig. 2 and Eq. (9)]. Input capacitance ( $C_{iss}$ ) of the aforementioned JFET's is about 5 pF at room temperature with  $V_{GS} = 0$  and  $V_{GD} = 10V$ . The average decrease of that capacitance with temperature between 300 and 120°K is 15%. The breakdown voltage ( $V_{DG}$ ) of the devices is in the range of 40 to 60V. Noise measurements on the silicon JFET's were reported by several researchers. Some report<sup>9, 13</sup> unexplained noise fluctuations with temperature in part of the tested units, with few units following Van der Ziel's theory. Others<sup>8</sup> show only noise variations following roughly Van der Ziel's theory. Typical noise (referred to input) achieved<sup>9</sup> around the optimum temperature was 0.3  $\mu V$  rms or an ENC of 60 electrons rms.

The commercial germanium JFET is a relative newcomer to the fast-expanding family of JFET's. To our knowledge there is only one type of germanium JFET manufactured in the United States. This is the p-channel TIX301 and its plastic-encapsulated version TIXM12, both produced by Texas Instruments Company. The parameters of these JFET's at room temperature are:

$$\begin{aligned} I_{dss}(V_{GS} = 0) &= 5 \text{ to } 25 \text{ mA} \\ \text{Transconductance, } g_m(V_{GS} = 0, V_{DS} = -8V) &= 7 \\ &\text{ mA/V typical} \\ \text{Input capacitance, } C_{iss}(V_{GS} = 0, V_{DS} = -8V) &= 15 \\ &\text{ pF max.} \\ \text{Breakdown voltage, } V_{DG} &= 20 \text{ to } 30V. \end{aligned}$$

The variation of  $I_{dss}$  with temperature as measured on three different units is shown in Fig. 4. The three units represent low, medium-, and high-current (and pinch-off voltage) devices. The current of the low-pinch-off-voltage device (No. 1) peaks around 100°K, but shows very little variation between liquid-helium and dry-ice temperatures. Device No. 2 shows a distinct plateau between 10 and 60°K. The current of No. 3 device peaks below liquid-helium temperature.

The variation of  $g_m$  with temperature is shown in Fig. 5. The behavior of No. 2 and No. 3 devices is as could be expected from the variation of their  $I_{dss}$  currents [Fig. 4 and Eq. (7) and (9)]. Device No. 1 exhibits a continuous increase of  $g_m$  also above 100°K. The reason for this behavior is the change in polarity of the temperature coefficient  $(\partial I_{dss} / \partial T)|_{V_{GS} = 0}$  for low-pinch-off-voltage devices. In the range 10 to 100°K, the temperature coefficient of  $I_{dss}$  for  $V_{GS} = 0$  is close to zero, while the one for  $V_{GS} = 0.1V$  is already positive.

Device No. 1 shows the highest  $g_m$  of the three recorded, but among the many other units

observed the highest  $g_m$  was 25 mA/V.<sup>14</sup> It was noticed that the TIX301's have a slightly higher  $g_m$  than the TIXM12's. The data of Figs. 4 and 5 were obtained with  $V_{DS} = -3V$ , as is necessary for low-noise operation of the FET. The transconductance of the three units at 10°K and  $V_{DS} = -5V$  is 20.1, 20.4, and 19.8 mA/V respectively.

The TIXM12 has low breakdown voltages, as might be expected, due to the lower breakdown field in germanium. These voltages decrease with temperature, and at liquid-helium temperature  $V_{DG}$  max. is between 15 and 25 V. The main disadvantage of the described germanium JFET's is their small operating range of drain-to-source voltages before avalanche-multiplication sets in. Figure 6 showing the  $I_d$ - $V_d$  curve of device No. 1 demonstrates the problem. The avalanche in the pinched-off channel becomes significant around  $V_{DS} = -6V$ .

The input capacitance of the TIXM12 at 4.2°K and  $V_{GS} = 0$ ,  $V_{DS} = -3V$  ranges from 10 to 15 pF. Gate leakage at that temperature is in the region of  $10^{-11}$  to  $10^{-12}$  A.

#### V. The Preamplifier

To demonstrate the low-noise properties of germanium JFET's the following preamplifier was assembled. The input stage of the preamplifier is shown in Fig. 7. It consists of two TIX301 (or TIXM12) units in cascade. Voltage-sensitive configuration is used and dc coupling between the detector and the input stage is employed, as these offer a high signal-to-noise ratio.<sup>9</sup> The FET's are operated at liquid-helium temperature with zero gate-to-source bias and  $V_{DS} = -2.5V$ . The input FET has lower saturation current, and its drain voltage is determined by the gate voltage of the second FET. The low  $V_{DS}$  prevents a large component of avalanche-type noise, but also causes relatively large junction capacitances. The high  $C_{rss}$  (~5 pF) forces us to use the cascade connection.

Excluding the input stage, the rest of the preamplifier is a conventional type of amplifier using bipolar transistors, which has been described elsewhere.<sup>9</sup> The only change made in this amplifier is the replacement of the npn transistor 2N1304 ( $Q_2$ ) by a pnp equivalent 2N1305 with the respective changes in bias polarities. Fast operation of the preamplifier using the germanium JFET input stage is possible by redesigning the rest of the preamplifier adequately.

The noise of the TIXM12 was measured with the help of the described preamplifier. The variation of the rms noise (referred to input) with temperature is shown in Fig. 8. The noise follows roughly Van der Ziel's theory between 10 and 90°K. From 90°K the noise starts to increase faster, which may indicate the growth of the gate's shot noise. The minimum noise was recorded at 10°K and was 0.2 $\mu$ V rms or ENC of about 40 electrons rms.

A remarkable property of the germanium JFET's is their almost perfect noise uniformity around liquid-helium temperature. Among 20 units tested the largest difference in noise was only 30%. This clearly contrasts the results obtained with silicon JFET's, where only 35% of tested units were found fit for low-noise amplifiers, and some units showed more than one order of magnitude higher noise. The minimum noise of the germanium FET's is obtained at the lowest attainable temperature (~5 to 10°K) as seen from Fig. 8 and confirmed in similar tests with different devices. This fact removes the need for temperature adjustment as used to obtain the optimum performance from silicon JFET's. The germanium FET's seem to have much smaller  $1/f$  noise. Low pinch-off voltage devices give slightly better signal-to-noise ratios and therefore those units are recommended for low-noise amplifiers. The selection process is therefore obviously simple as compared to the one used for silicon FET's.

#### VI. Experimental Results.

The preamplifier performance was checked with a pulse generator and radioactive sources. The conventional pulse generator test was carried out using a 0.5-pF testing capacitor. The resolution of the preamplifier for zero external capacitance is 0.28 keV FWHM (Ge) with a slope of 0.018 keV/pF. The very low sensitivity to external capacitance (of the detector) is a result of the relatively high input capacitance of the FET's, which on the other hand prevents the achievement of higher signal-to-noise ratios.

The preamplifier described was used with a low-capacitance (2-pF) LRL-Berkeley-type lithium-drifted silicon detector. The detector was operated at 110°K in a vacuum of  $5 \times 10^{-7}$  mm Hg and with a bias voltage of 1 kV. The details of detector mounting and its isolation from ground are described elsewhere.<sup>15</sup> The pulse-shaping time constants of the main amplifier were 5  $\mu$ sec integration and differentiation.

The preamplifier assembly was checked for actual resolution with x rays of  $^{55}\text{Mn}$  and  $^{241}\text{Am}$ . The pulse-height analyzer spectra are shown in Figs. 9 and 10. The  $K_\alpha$  and  $K_\beta$  lines of  $^{55}\text{Mn}$  (Fig. 9), only 0.6 keV apart, are resolved and measured with 0.37-keV resolution. The spectrum of  $^{241}\text{Am}$  (Fig. 10) shows the fine structure of this source; some of the very weak lines ( $L_\eta$ ,  $L_\beta$ , and  $L_\gamma$ ) are resolved from the background noise. The  $L_\alpha$  line ( $L_{\alpha_1} = 13.96$  keV,  $L_{\alpha_2} = 13.78$  keV) was measured with 0.42-keV resolution, and the  $L_{\gamma_1}$  and  $L_{\gamma_6}$  lines (0.68 keV apart) were resolved. The  $L_{\beta_1}$  and  $L_{\beta_2}$  lines (0.81 keV apart), previously barely resolved,<sup>9</sup> now show a 2:1 peak-to-valley ratio.



## VII. Conclusions

The low-noise properties of germanium JFET's, stemming from the properties of germanium at cryogenic temperatures, were described. That relatively new device was compared with silicon JFET's used extensively in low-noise preamplifiers. The advantages of the germanium device are higher signal-to-noise ratio available at liquid-helium temperature, a simple selection process, and no need for temperature adjustment.

A preamplifier using commercial germanium FET's in its input stage was built. Pulse generator resolution for zero external capacitance is 0.28 keV FWHM (Ge) with a slope of 0.018 keV/pF. These results were obtained in spite of the low breakdown voltage and high input capacitance of the only available type of FET's. Therefore further improvements of resolution are expected with the technological progress in fabrication of germanium FET's. Comparing the mobilities of p and n type germanium, we see that n-channel devices may offer additional advantages.

The described preamplifier was tested with a low-capacitance, lithium-drifted silicon detector, and low-energy x rays were consistently measured with 0.37-keV resolution. The use of the described preamplifier in conjunction with germanium detectors operated below 77°K is currently being investigated.

Concluding, we can say that the germanium JFET has proved to be a very low-noise device when operated at liquid-helium temperature. We believe the same is true for other low-energy gap materials, especially such high-mobility materials as InSb, which may serve as the basis for future low-noise devices.

## Acknowledgment

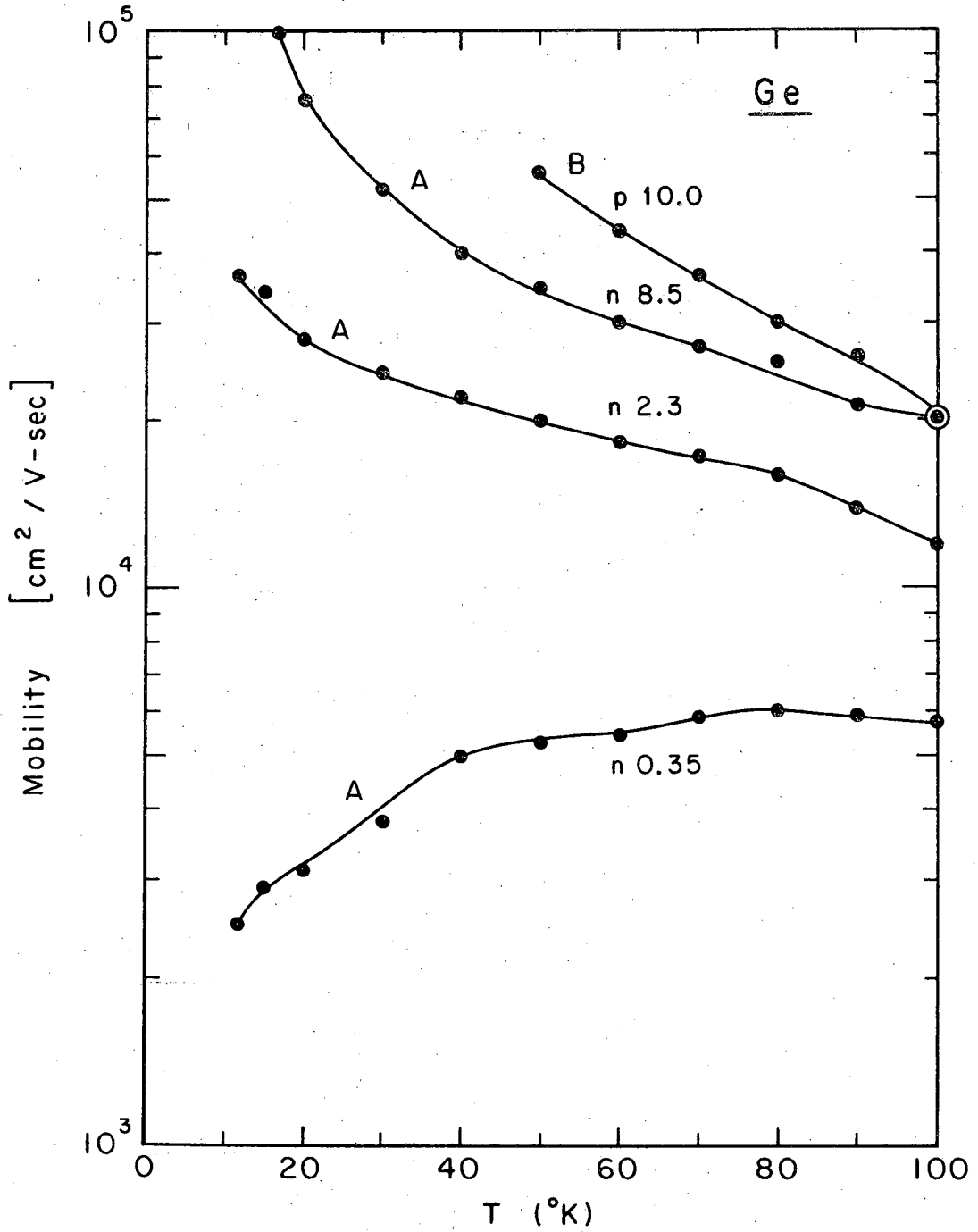
The authors would like to thank W. L. Crowder for his technical assistance.

## References

1. R. L. Chase, W. A. Higinbotham, and G. L. Miller, IRE NS-8, No. 1, 147 (1961).
2. J. L. Blankenship, IEEE NS-11, No. 3, 373, (1964).
3. A. W. Pryor, Nucl. Instr. Methods 6, 164 (1960).
4. T. L. Emmer, IRE NS-9, No. 3, 305 (1962).
5. L. G. Jonasson, Nucl. Instr. Methods 26, 104 (1964).
6. V. Radeka, Brookhaven National Laboratory Report BNL-6953 (1963).
7. E. Elad, Nucl. Instr. Methods 37, 327 (1965).
8. K. F. Smith and J. E. Cline, IEEE NS-13, No. 3, 468 (1966).
9. E. Elad and M. Nakamura, IEEE NS-14, No. 1, 523 (1967).
10. P. Aigram, Selected Constants Relative to Semiconductors (Pergamon Press, London, England, 1961).
11. S. Wang, Solid State Electronics (McGraw Hill, New York 1966), p. 149.
12. Van der Ziel, Proc. IRE 50, 1808 (1962).
13. T. V. Blalock, IEEE NS-13, No. 3, 457 (1966).
14. E. Elad and M. Nakamura, Lawrence Radiation Laboratory Report UCRL-17632, June 1967 (to be published in Nucl. Instr. Methods).
15. E. Elad and M. Nakamura, Nucl. Instr. Methods 41, 161 (1966).
16. E. M. Conwell, Proc. IRE 40, 1327 (1952).
17. F. J. Morin, Phys. Rev. 93, 62 (1954).
18. G. A. Swartz, J. Phys. Chem. Solids 12, 245 (1960).
19. F. J. Morin and J. P. Maita, Phys. Rev. 96, 28 (1954).

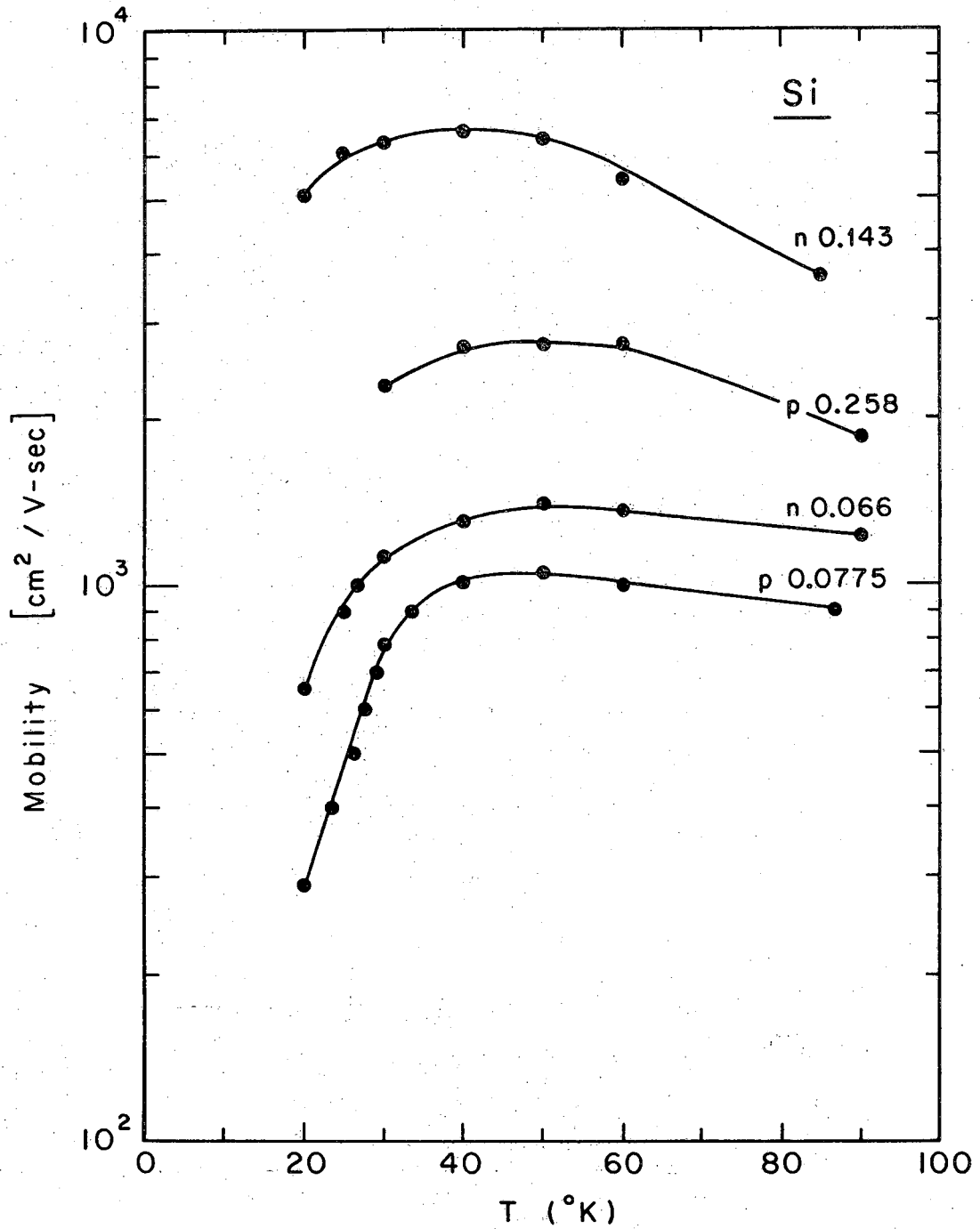
Figure Captions

- Fig. 1a. Mobility of germanium at cryogenic temperatures. (A) Conwell,<sup>16</sup> (B) Morin.<sup>17</sup> The resistivity of each sample at room temperature is indicated.
- Fig. 1b. Mobility of silicon (after Swartz.<sup>18</sup>)
- Fig. 2. Conductivity of germanium and silicon at cryogenic temperatures. Ge: Conwell,<sup>16</sup> Si: Morin and Maita.<sup>19</sup>
- Fig. 3. Transconductance of a silicon JFET (2N3823) at cryogenic temperatures.
- Fig. 4. Saturation current of TIXM12 versus temperature.
- Fig. 5. Transconductance of TIXM12 versus temperature.
- Fig. 6.  $I_d - V_d$  characteristic of TIXM12 at 4.2°K.
- Fig. 7. The input stage of the preamplifier.
- Fig. 8. Root-mean-square noise of TIXM12 versus temperature.
- Fig. 9. Spectrum of <sup>55</sup>Mn x rays. Energy in keV.
- Fig. 10. Spectrum of <sup>241</sup>Am x rays. Energy in keV.



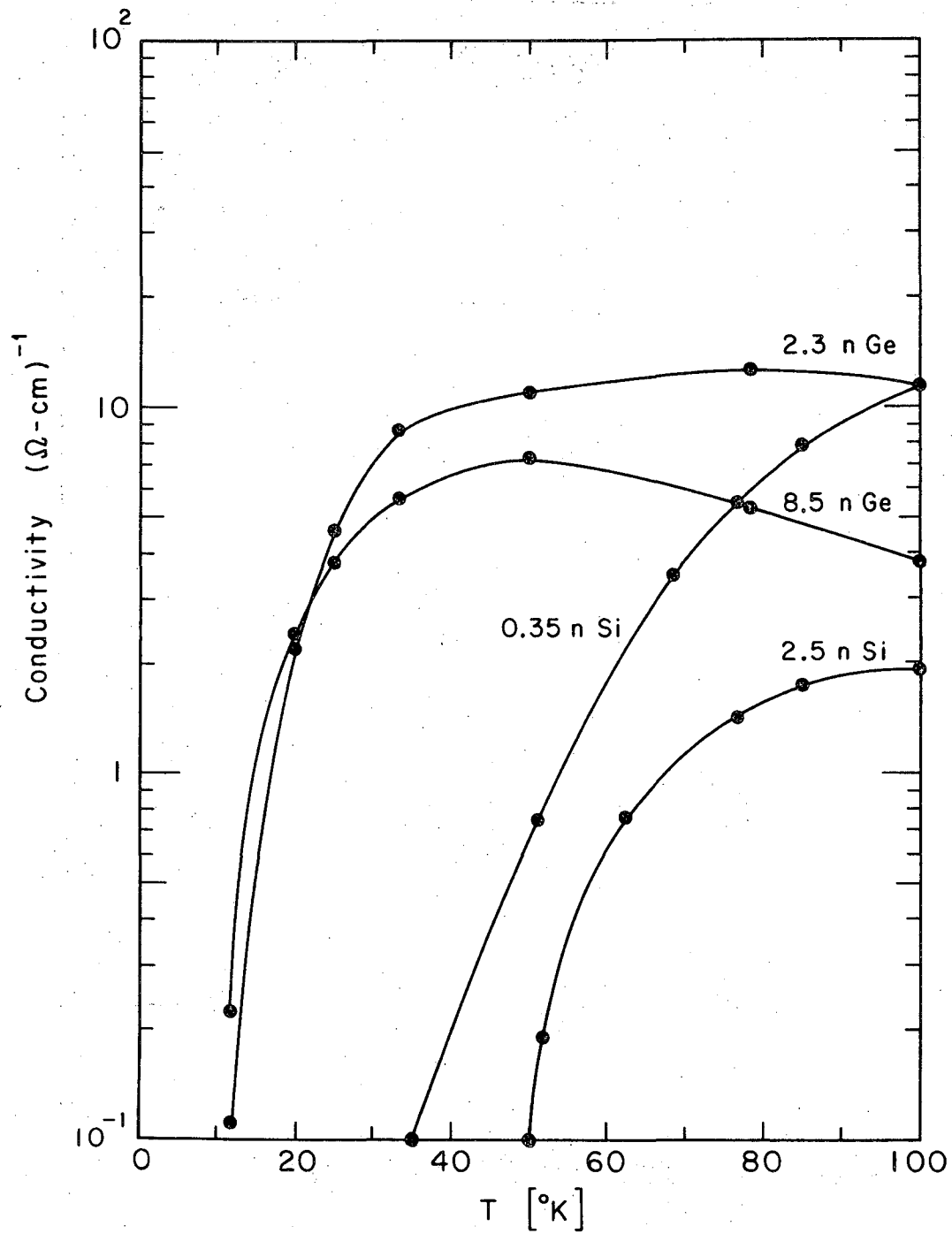
XBL679-5282

Fig. 1a



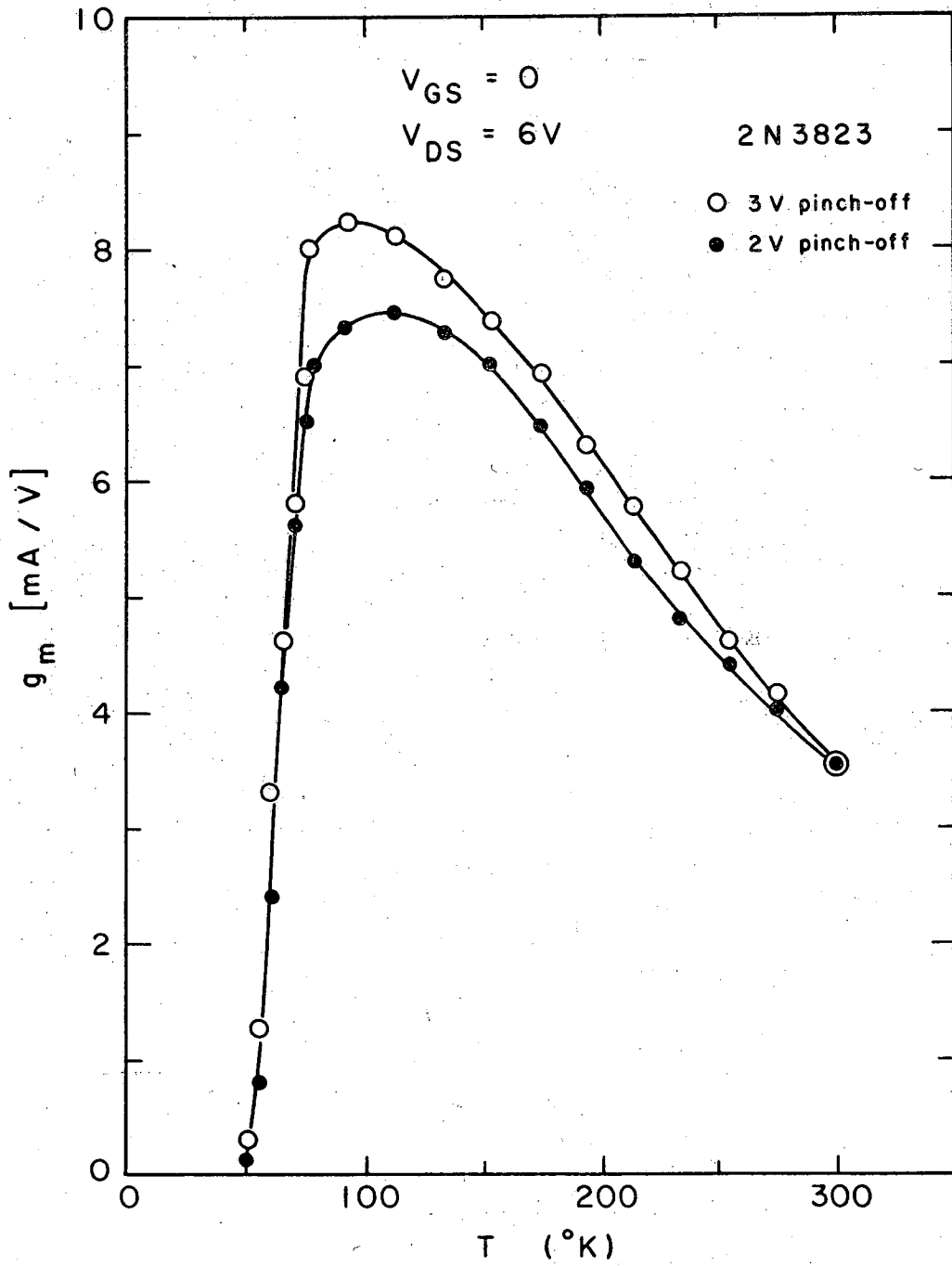
XBL679-5283

Fig. 1b



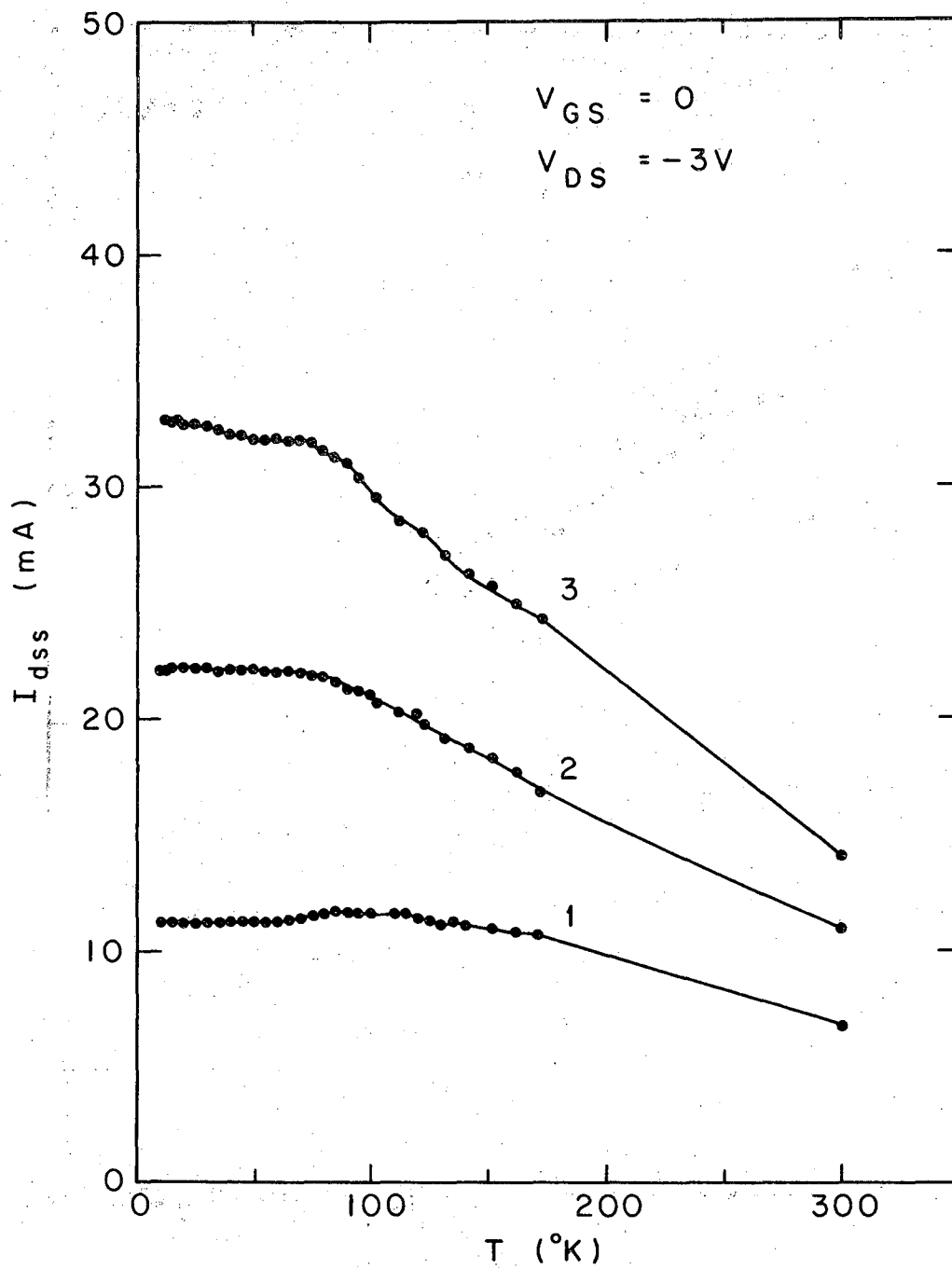
XBL679-5284

Fig. 2



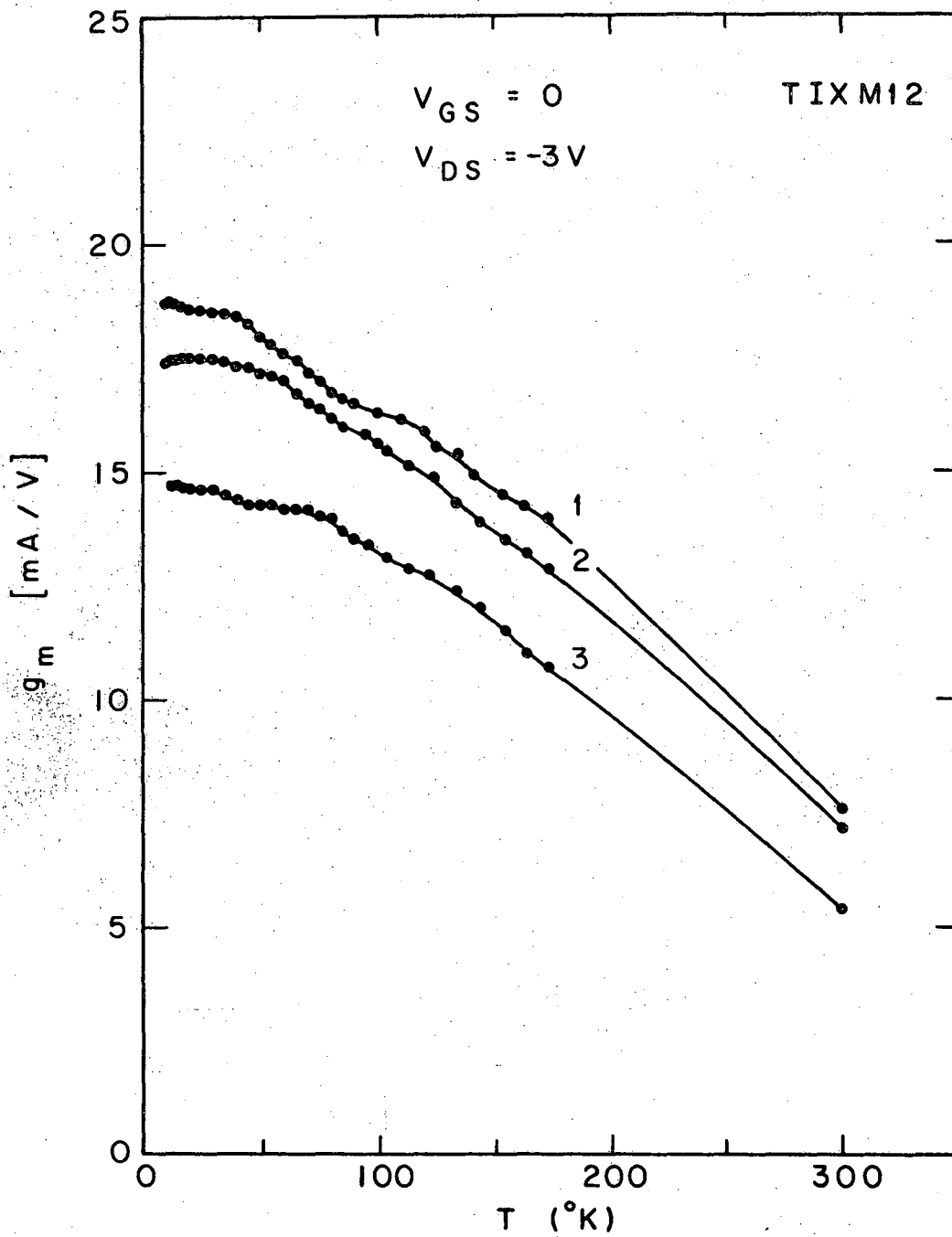
XBL679-5285

Fig. 3



XBL679-5286

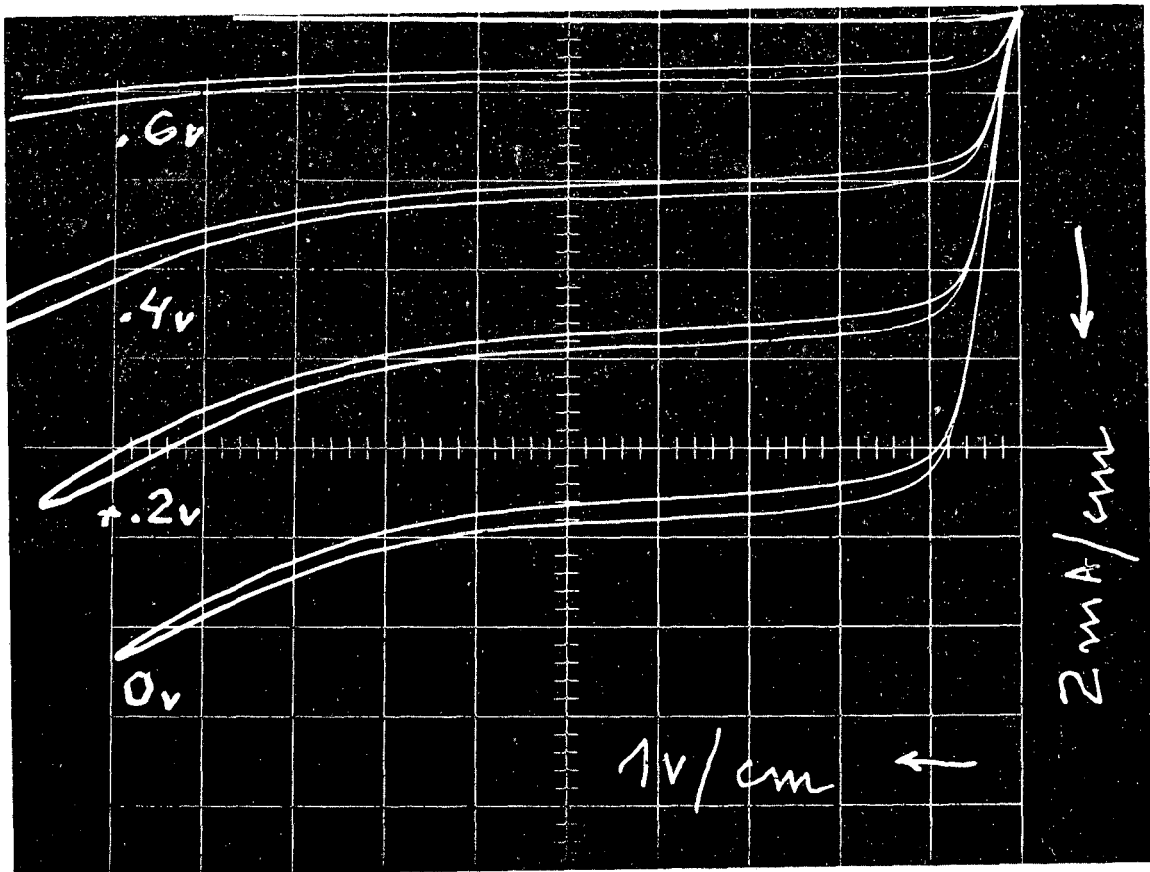
Fig. 4



XBL679-5287

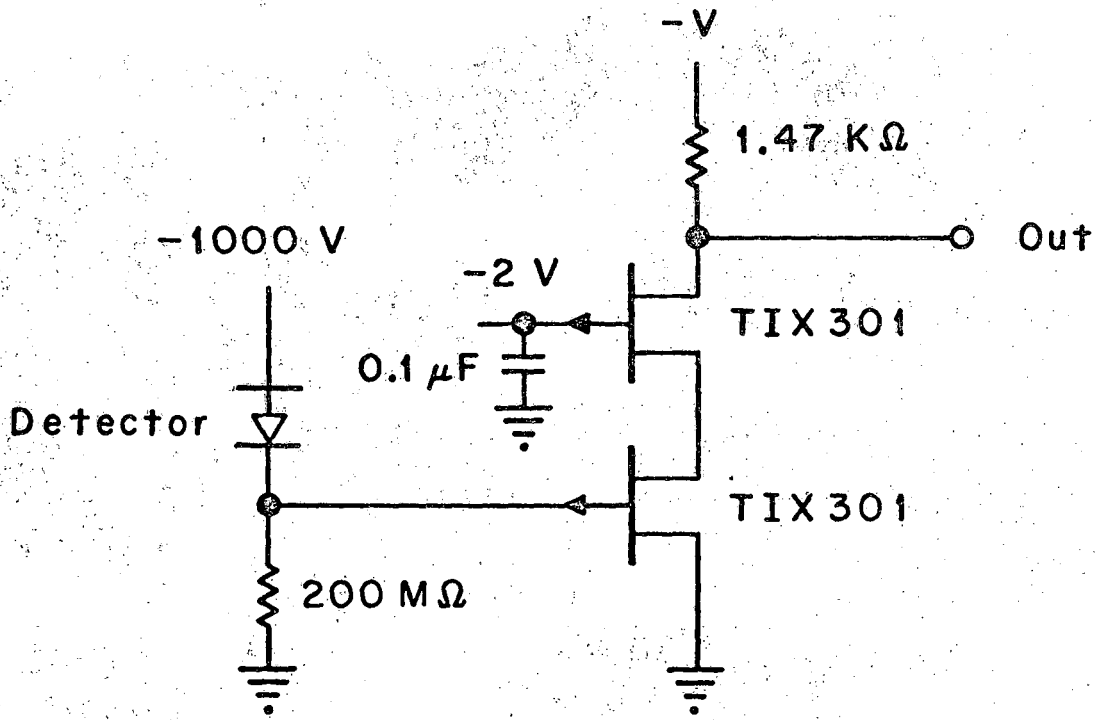
Fig. 5





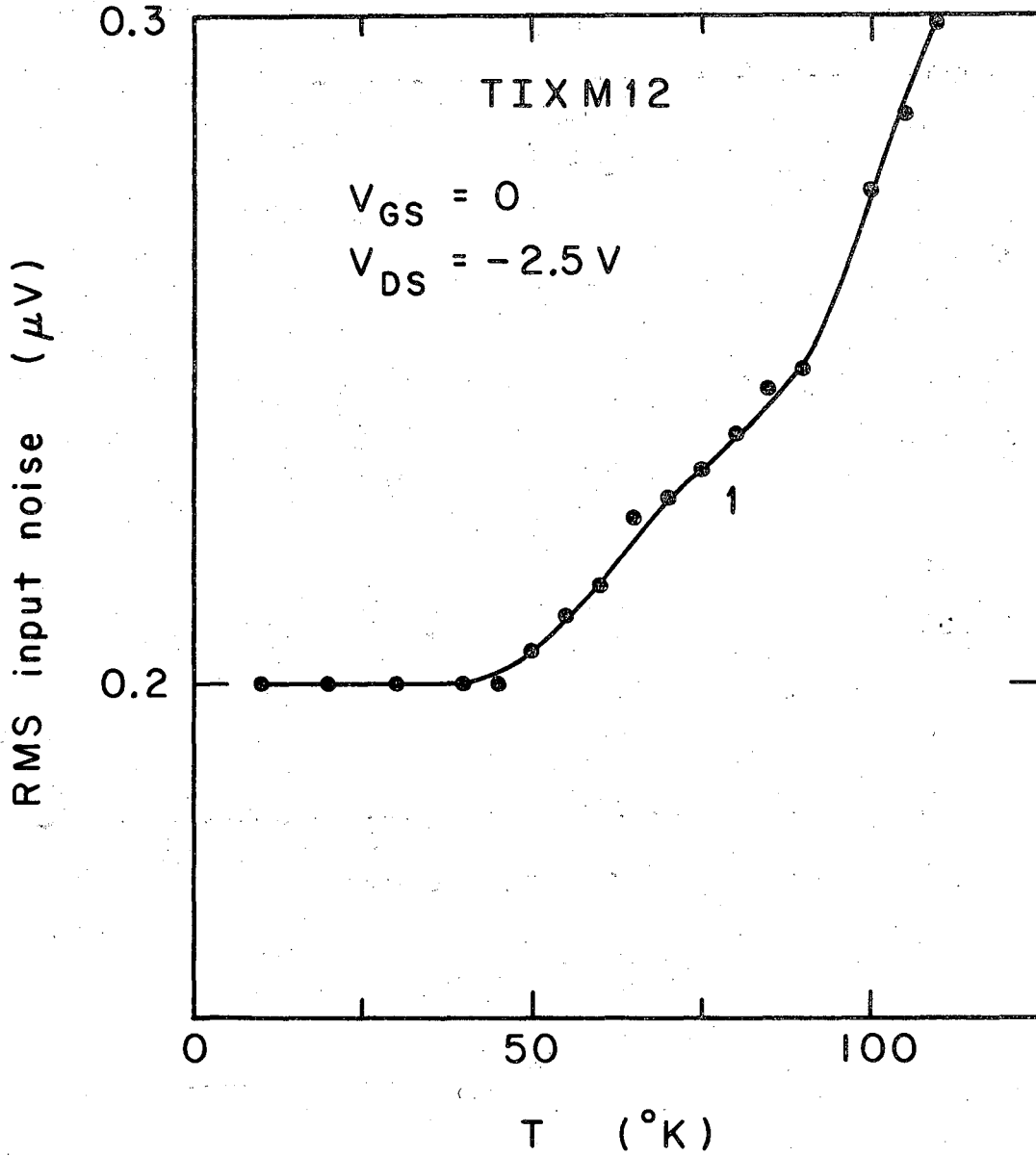
XBB 670-5735

Fig. 6



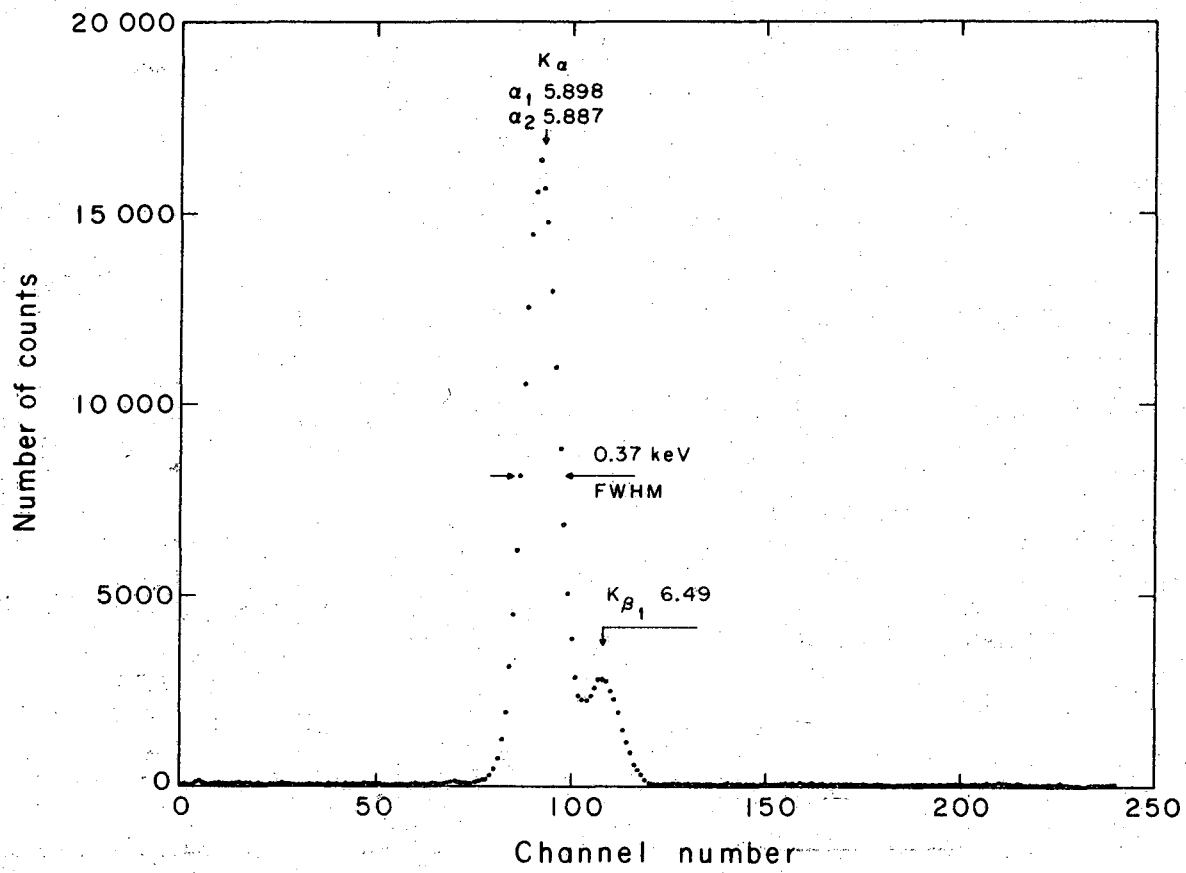
XBL 676-3383

Fig. 7



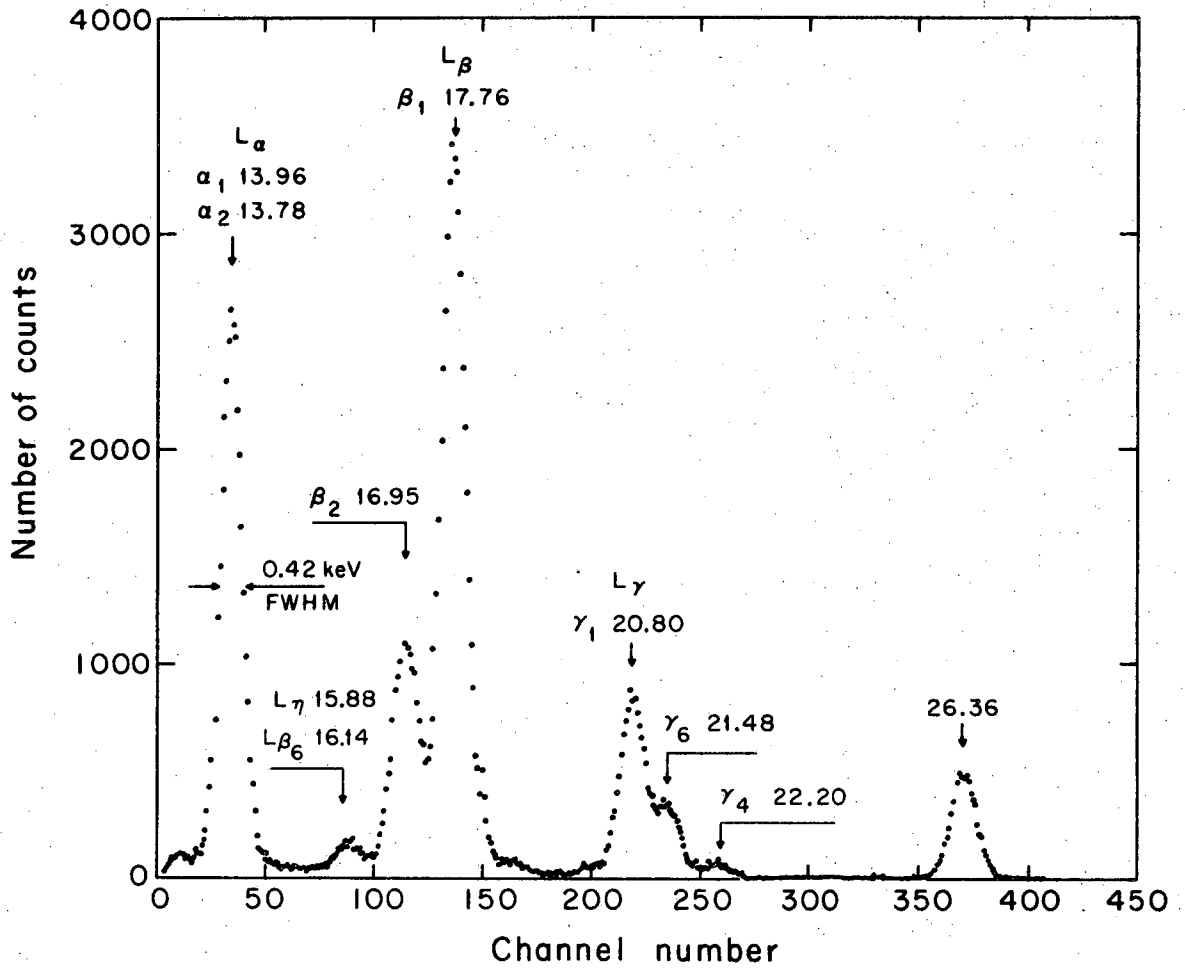
XBL679-5288

Fig. 8



XBL676-3227

Fig. 9



XBL676-3228

Fig. 10

This report was prepared as an account of Government sponsored work. Neither the United States, nor the Commission, nor any person acting on behalf of the Commission:

- A. Makes any warranty or representation, expressed or implied, with respect to the accuracy, completeness, or usefulness of the information contained in this report, or that the use of any information, apparatus, method, or process disclosed in this report may not infringe privately owned rights; or
- B. Assumes any liabilities with respect to the use of, or for damages resulting from the use of any information, apparatus, method, or process disclosed in this report.

As used in the above, "person acting on behalf of the Commission" includes any employee or contractor of the Commission, or employee of such contractor, to the extent that such employee or contractor of the Commission, or employee of such contractor prepares, disseminates, or provides access to, any information pursuant to his employment or contract with the Commission, or his employment with such contractor.

